Journal of Alloys and Compounds 755 (2018) 10–14

Contents lists available at ScienceDirect

Journal of Alloys and Compounds

journal homepage: http://www.elsevier.com/locate/jalcom

Coexistence of charge density wave and incommensurate antiferromagnetism in the cubic phase of $DyGe_{2.85}$ synthesised under high pressure

D.A. Salamatin [a, b, c, *], V.A. Sidorov [a], S.E. Kichanov [d], A. Velichkov [c, f], A.V. Salamatin [c], L.N. Fomicheva [a], D.P. Kozlenko [d], A.V. Nikolaev [e, b], D. Menzel [g], M. Budzynski [h], A.V. Tsvyashchenko [a, **]

[a] Vereshchagin Institute for High Pressure Physics, RAS, 142190 Troitsk, Moscow, Russia
[b] Department of Problems of Physics and Energetics, Moscow Institute of Physics and Technology, 141700 Dolgoprudny, Russia
[c] Dzelepov Laboratory of Nuclear Problems, Joint Institute for Nuclear Research, 141980 Dubna, Russia
[d] Frank Laboratory of Neutron Physics, Joint Institute for Nuclear Research, 141980 Dubna, Russia
[e] Skobeltsyn Institute of Nuclear Physics Lomonosov Moscow State University, 119991 Moscow, Russia
[f] Institute for Nuclear Research and Nuclear Energy, 1784 Sofia, Bulgaria
[g] Institute of Condensed Matter Physics, TU Braunschweig, 30816 Braunschweig, Germany
[h] Institute of Physics, M. Curie-Sklodowska University, 20-031 Lublin, Poland

ARTICLE INFO

Article history:
Received 14 December 2017
Received in revised form
25 April 2018
Accepted 28 April 2018
Available online 1 May 2018

Keywords:
High pressure
TDPAC
Neutron powder diffraction
Charge density wave
Incommensurate magnetism
Rare earth compound

ABSTRACT

A novel metastable phase of $DyGe_{2.85}$ synthesised in the $AuCu_3$-structure under high pressure, has been studied by means of the magnetic susceptibility and electrical resistivity measurements (under the pressure $P \leq 3.1$ GPa), neutron powder diffraction and time-differential γ-γ perturbed angular correlations (TDPAC) using ^{111}Cd nuclear probes. Two distinct phase transitions have been found in this compound as the temperature is lowered. We assign the first transition occurring at the temperature $T_{CDW} = 80$ K with charge density wave formation and the second transition at $T_N \approx 18$ K with an antiferromagnetic spiral ordering of Dy magnetic moments, and discuss a close relationship between them.

1. Introduction

The interplay and interconnections between various interactions, which lead for example to the coexistence of magnetism and superconductivity [1,2], charge density wave (CDW) and superconductivity [3], ferroelectric and magnetic order in multiferroics [4], and different types of magnetic ordering [5,6], represent one of the most intriguing problems of the modern solid state physics.

In particular, recent studies have focused on physics of CDW in rare-earth compounds and its influence on periodic lattice distortions (PLD) and magnetic ordering [7–12]. In Refs. [8,9,11,12] it has been shown that CDW-PLD can coexist with antiferromagnetic (AFM) ordering, although the nature of this coexistence is not well understood.

The question about the formation of CDW in intermetallic compounds is also relevant [13]. Earlier, a series of new intermetallic compounds of the $AuCu_3$ cubic structure – $REGe_{2.85}$ where RE is a rare earth element (Tb, Dy or Yb) – has been synthesized at high pressure [19]. In $TbGe_{2.85}$ belonging to this series, two phase transitions have been reported in Ref. [20]. The first transition at the temperature $T_{CDW} = 145$ K has been related with the CDW transition while the second at $T_N = 19$ K with an AFM ordering, where Tb magnetic moments form incommensurate spiral [20]. While the

* Corresponding author. Vereshchagin Institute for High Pressure Physics, RAS, 142190 Troitsk, Moscow, Russia.
** Corresponding author.
E-mail addresses: dasalam@gmail.com (D.A. Salamatin), tsvyash@hppi.troitsk.ru (A.V. Tsvyashchenko).

https://doi.org/10.1016/j.jallcom.2018.04.319
0925-8388/

Neel temperature T_N in $TbGe_{2.85}$ has been found to be approximately independent of the pressure, T_{CDW} decreases with increasing pressure, until the CDW transition is completely suppressed at $P \geq 2.6$ GPa. The neutron powder diffraction at low temperature and high pressure reveals the appearance of the second magnetic commensurate phase at $P \geq 1.2$ GPa. These experimental findings imply that CDW and the AFM structure in $TbGe_{2.85}$ are closely related, but the microscopic mechanism behind this effect is little understood.

To clarify the interconnection between CDW and magnetic ordering, we have undergone an experimental examination of $DyGe_{2.85}$, belonging to the same series of the cubic rare-earth compounds $REGe_{2.85}$ as $TbGe_{2.85}$. It should be noted that most of the $AuCu_3$ rare-earth compounds have commensurate magnetic structures [14–16] and only few of them display incommensurate magnetic ordering [15,17,18]. In this paper we present our experimental data and analysis, performed by macro-methods such as magnetic susceptibility and electrical resistivity, and by nuclear methods including time-differential γ-γ perturbed angular correlations (TDPAC) and neutron powder diffraction (NPD).

2. Experiment details

Polycrystalline samples of $DyGe_{2.85}$ were synthesised at a pressure of 8 GPa as described in Ref. [22].

The refinement of the x-ray diffraction (XRD) data have shown that the polycrystalline samples of $DyGe_{2.85}$ have the $AuCu_3$ structure ($Pm\bar{3}m$ space group (No. 221)) with the lattice constant $a = 4.286(4)$ Å at room temperature and ambient pressure [19].

The electrical resistivity was measured by four probe method. The sample and the pressure sensor (Pb) were placed in teflon ampoule filled with pressure transmitting liquid. The clamped toroid-type cell was used to generate high pressures [23].

The magnetic susceptibility $\chi(T)$ of the sample was obtained using SQUID magnetometer.

The parameters of hyperfine interactions were obtained by the TDPAC spectroscopy on *In*/*Cd* nuclear probes. During the sample synthesis the probes were inserted into the $DyGe_{2.85}$ lattice, where as shown in Ref. [19] they occupied sites of Ge vacancies. Experimental data were analyzed with the DEPACK software [26]. Details of the TDPAC method and the used spectrometer are described in Refs. [24,25].

NPD measurements were conducted on the DN-6 diffractometer at the IBR-2 high-flux pulsed reactor [Frank Laboratory of Neutron Physics, Joint Institute for Nuclear Research (JINR), Dubna, Russia] [27]. NPD patterns were recorded at ambient pressure and the following temperatures: $T = 300, 20, 16, 12, 8$ and 4 K. The low temperature was achieved with a closed-cycle helium cryostat. Diffraction patterns were collected at scattering angle $2\Theta = 90^\circ$ with resolution $\Delta d/d = 0.011$. The exposition time for one record was about 20 h. NPD patterns were analyzed with the Rietveld method using FULLPROF software [28].

3. Results and discussion

Temperature dependencies of the measured resistivity $\rho(T)$ of $DyGe_{2.85}$ at various pressures are shown in Fig. 1; at ambient conditions $\rho(300K)$ $90\mu\Omega-$ cm. These plots at $T \geq 80$ K have a typical metallic behaviour linear in *T*, and the resistivity drops with applied external pressure. One of the reasons for this drop is the increase in the density of states at the Fermi level for $DyGe_{2.85}$.

The temperature coefficient of resistivity at $P = 0$ and 3.1 GPa is approximately the same which can point to an unaltered value of the electron-phonon coupling constant in $DyGe_{2.85}$ in this pressure range.

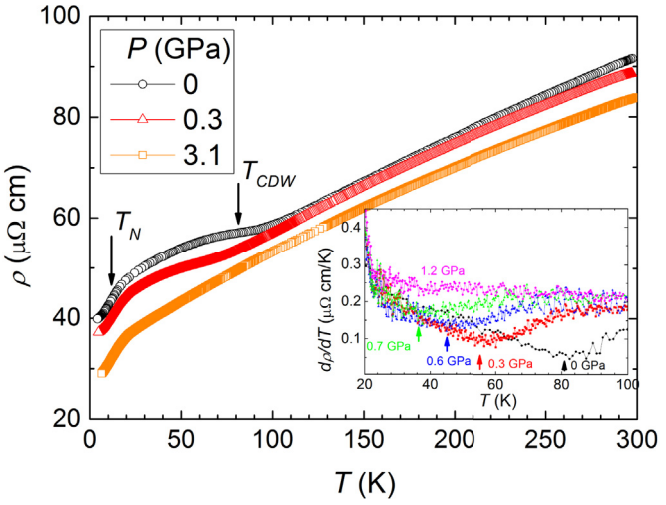

Fig. 1. Resistivity $\rho(T)$ of $DyGe_{2.85}$ versus temperature at different external pressures. Inset: $\frac{d\rho}{dT}$ versus T at different pressures for $DyGe_{2.85}$. The arrows mark the CDW anomaly.

The most important feature of the normal pressure plot is the appearance of two anomalies, at $T_{CDW} = 80$ K and $T_N \approx 20(2)$ K. Below we will demonstrate that the first anomaly (at T_{CDW}) can be connected with a CDW formation, while the second smooth transition (at T_N) with magnetic ordering. Exact values of T_{CDW} have been determined from the position of the minimum of $\frac{d\rho}{dT}(T)$ (see inset of Fig. 1). At ambient pressure $T_{CDW} = 80$ K.

With the application of pressure, the temperature T_{CDW} decreases at a rate of $\frac{dT_{CDW}}{dP} \approx -65$ K/GPa and the CDW anomaly of resistivity is not observed at pressures above $P = 1$ GPa. In contrast to T_{CDW}, T_N is approximately pressure independent. We observed approximately the same rate of $\frac{dT_{CDW}}{dP}$ for $TbGe_{2.85}$ and T_N was also pressure independent in this pressure range [21] (see Fig. 2).

The two anomalies found in resistivity, manifest themselves in

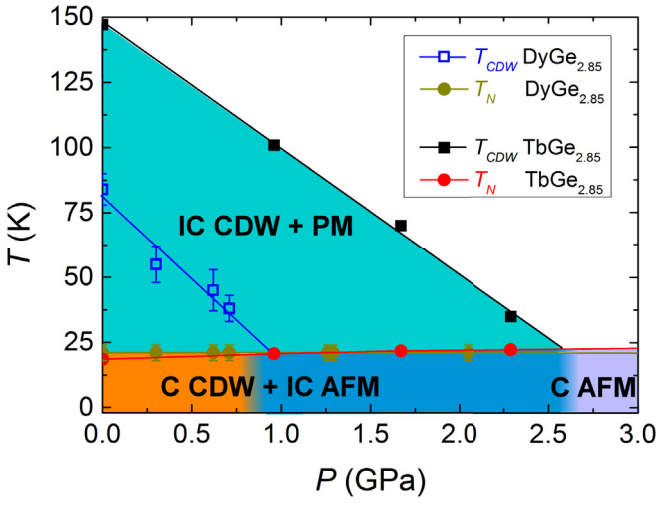

Fig. 2. The phase diagram for $TbGe_{2.85}$ and $DyGe_{2.85}$. Antiferromagnetic transition temperature T_N and CDW transition temperature T_{CDW} versus pressure. The region of turquoise color highlights the region with incommensurate (IC) CDW and paramagnetism (PM); orange color highlights the region with commensurate (C) CDW and IC AFM for $DyGe_{2.85}$; blue color highlights the region with C CDW and IC AFM for $TbGe_{2.85}$ (no CDW transition in $DyGe_{2.85}$); purple color highlights the region with C AFM for $TbGe_{2.85}$. (For interpretation of the references to color in this figure legend, the reader is referred to the Web version of this article.)

all other experiments, in particular, in magnetic susceptibility $\chi(T)$, Fig. 3. In Fig. 3 we also plot $\chi^{-1}(T)$ with the Curie-Weiss fit (straight line), whose parameters are quoted in the inset. As in $TbGe_{2.85}$ [20], one can see a small deviation from the Curie-Weiss law, which sets in at approximately $T \sim 100$ K (which is slightly higher the anomaly on the $\rho(T)$ curve) and continues at lower temperatures. At $T_N = 18(1)$ K there is a magnetic transition to AFM phase, with the effective magnetic moment of dysprosium, $\mu_{eff} = 10.60\ \mu_B$. This magnetic moment is consistent with the value of the Dy^{3+} free ion, $\mu_{Dy^{3+}} = 10.62\ \mu_B$.

The Néel temperature (T_N) for $TbGe_{2.85}$ is 1 K higher than that for $DyGe_{2.85}$. This is consistent with the well-known dependence of T_N on de Gennes factor $(g_J - 1)^2 J(J+1)$ (which is 10.5 for Tb and 7.08 for Dy). This dependence however is weak, which is an indication that in addition to the Ruderman - Kittel - Kasuya - Yosida (RKKY) coupling some other interactions can be involved.

Peculiarities of the electronic and magnetic structure of $DyGe_{2.85}$ have been also studied by TDPAC spectroscopy, whose spectra $R(t)$ at $T = 300, 30$ and 4 K at ambient pressure are presented in Fig. 4. The $T = 300$ K spectrum is refined with the single quadrupolar frequency $\nu_Q = 39.6(5)$ MHz (the electric field gradient (EFG) $V_{zz} = \frac{h\nu_Q}{eQ} = 1.98(2)$ V/sm^2) and a small asymmetry parameter $\eta = (V_{xx} - V_{yy})/V_{zz} = 0.06(8)$. The Ge lattice site in the perfect cubic structure is axially symmetric, which implies $\eta = 0$, but in our case the presence of vacancies in Ge sites and also inserted *In/Cd* probes lead to a small deviation from the axial symmetry, resulted in a small value of $\eta \neq 0$. It is worth mentioning that approximately the same value of η has been observed for other high pressure cubic compounds with Yb and Tb at normal conditions [19].

The $T = 30$ K TDPAC spectrum is fitted with single quadrupolar frequency $\nu_Q = 39.8(5)$ MHz ($V_{zz} = 1.98(2)$ V/sm^2) and $\eta = 0.2(1)$. At this temperature a small frequency broadening was observed, $\delta = 0.14(3)$. Notice, that in the AFM phase (i.e. at $T < T_N$) the TDPAC spectrum is very different from that in the paramagnetic phase, see Fig. 4. Thus, the $T = 4$ K spectrum has been fit with two quadrupolar frequencies: $\nu_{Q1} = 10(1)$ MHz ($V_{zz} = 0.49(4)$ V/sm^2), $\nu_{Q2} = 16(1)$ MHz ($V_{zz} = 0.78(4)$ V/sm^2) and two Larmor precession frequencies $\nu_{L1} = 9(1)$ MHz (hyperfine magnetic field $B_{hf1} = \frac{h\nu_L}{g\mu_N} = 3.9(4)$ T), $\nu_{L2} = 6(1)$ MHz ($B_{hf2} = 2.4(4)$ T) with the approximate occupation ratio 2:1. This indicates that below the AFM transition temperature Ge sites become electronically and magnetically nonequivalent.

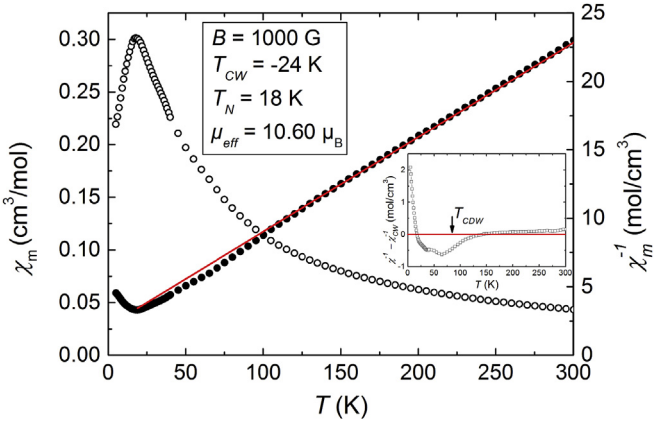

Fig. 3. The magnetic susceptibility $\chi(T)$ (empty circles) and inverse magnetic susceptibility $\chi^{-1}(T) = \frac{1}{\chi(T)}$ (filled circles) of $DyGe_{2.85}$ versus temperature at ambient pressure. The red line is Curie-Weiss approximation of $\chi^{-1}(T)$. The data are obtained in a field of 1000 G. Inset: Difference between the experimental data for $\chi^{-1}(T)$ and the Curie-Weiss fit ($\chi^{-1}_{CW}(T)$). The arrow marks the CDW anomaly. (For interpretation of the references to color in this figure legend, the reader is referred to the Web version of this article.)

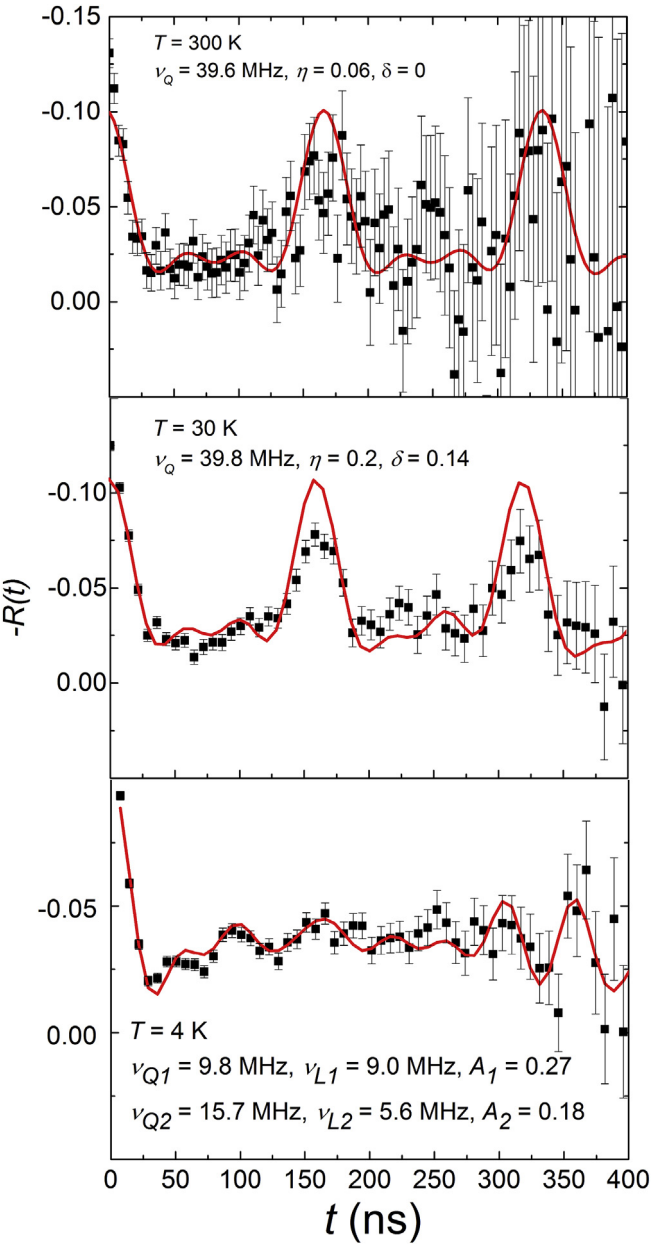

Fig. 4. TDPAC spectra $R(t)$ of ^{111}Cd probes in $DyGe_{2.85}$ (black squares) at $T = 300, 30$ and 4 K at ambient pressure, with their fits (red lines) and some fitting parameters (quadrupolar frequency ν_Q, asymmetry parameter η, frequency distribution δ, Larmor frequency ν_L and amplitudes A.). (For interpretation of the references to color in this figure legend, the reader is referred to the Web version of this article.)

To account for the existence of a single broad quadrupolar frequency line ν_Q above the T_N (i.e. in paramagnetic phase) and two sharp quadrupolar frequencies ν_{Q1} and ν_{Q2} below T_N (i.e. in the AFM phase), we are led to conclude that CDW is accompanied by an incommensurate lattice modulation in the paramagnetic phase and a commensurate lattice modulation in the magnetic phase.

Further refinement of the magnetic order in the low-temperature AFM phase has been performed with neutron powder diffraction studies of the $DyGe_{2.85}$ sample. The room-temperature analysis has confirmed that the sample has single phase with the space group $Pm\bar{3}m$ and the lattice constant

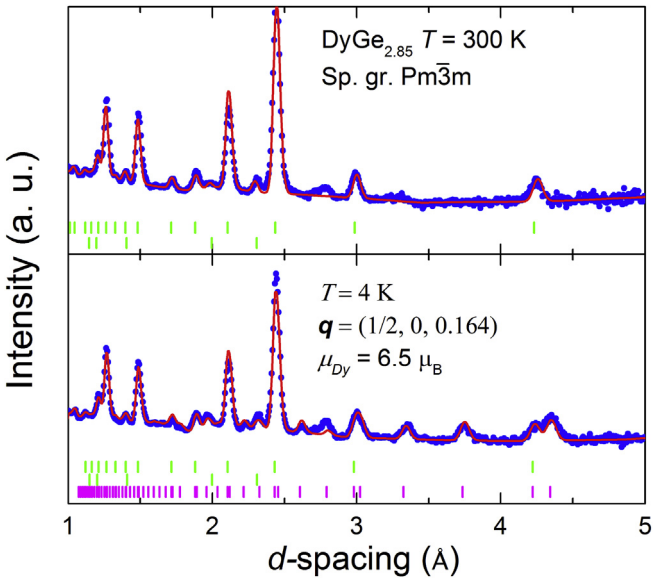

Fig. 5. Refined neutron powder diffraction pattern of $DyGe_{2.85}$ at 300 and 4 K at ambient pressure. Experimental points (blue points) and calculated profiles (red lines) are shown. Tick marks at the bottom represent the calculated positions of nuclear peaks for the $Pm\bar{3}m$ space group (upper row, green color), peaks from aluminum container (medium row, green color) and peaks from incommensurate magnetic phase (lower row, magenta color). (For interpretation of the references to color in this figure legend, the reader is referred to the Web version of this article.)

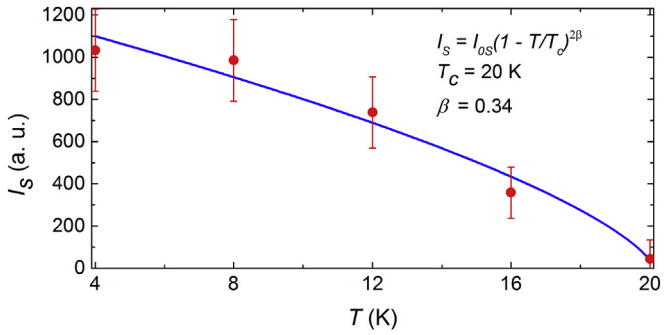

Fig. 6. Integral intensity I_S of the magnetic peak $q = (q_x, -1+q_y, -1+q_z)$ versus temperature (red points). Blue line is the $I_{0S}(1-T/T_C)^{2\beta}$ approximation ($I_{0S} = 1279$, $T_C = 20$ K, $\beta = 0.34$). (For interpretation of the references to color in this figure legend, the reader is referred to the Web version of this article.)

$a = 4.285(1)$ Å, Fig. 5. These data are in good agreement with previous XRD study [19].

At temperatures $T < 16$ K new peaks appear in the NPD patterns which have been fit using a model of incommensurate spiral structure of Dy magnetic moments. At $T = 4$ K the fit results in the wave vector $\mathbf{q} = (1/2, 0, 0.164(1))$ and the Dy magnetic moment $\mu_{Dy} = 6.5(1)\ \mu_B$, Fig. 5. It should be noted that approximately the same wave vector was found for $TbGe_{2.85}$ compound [20]. Therefore we conclude that the modulation period of CDW-PLD in both $DyGe_{2.85}$ and $TbGe_{2.85}$ is approximately the same which stabilizes the periodicity of magnetic modulation in *z*-direction. The obtained magnetic moment of Dy from NPD is almost half of the value for free ion Dy^{3+}. This deviation is probably caused by crystalline field effects (CFE) and molecular field. It is also in agreement with *ab initio* density functional calculations for isostructural compound $DySn_3$ [29], which give $\mu_{Dy} \approx 4.7\ \mu_B$.

It should be also noted that at $T = 4$ K we have not observed a symmetry change of the room temperature crystallographic structure ($AuCu_3$), only a small decrease of the lattice constant has been detected, $a = 4.248(2)$ Å.

Finally, Fig. 6 shows the temperature evolution of the integral intensity I_S of the magnetic peak $(q_x, -1+q_y, -1+q_z)$, appeared at low temperatures. This dependency has been approximated by the function $I_{0S}(1-T/T_C)^{2\beta}$ with the critical temperature $T_C = 20(3)$ K and the critical exponent $\beta = 0.34(8)$. The critical temperature virtually coincides with the values obtained from resistivity and magnetic susceptibility measurements.

4. Conclusion

Thus, both electrical resistivity $\rho(T)$ and magnetic susceptibility $\chi(T)$ in $DyGe_{2.85}$ display two anomalies at temperatures $T_{CDW} = 80$ K and $T_N \approx 18$ K. The first anomaly is associated with the formation of CDW while the second with an AFM ordering. The measurements of $\rho(T)$ at different external pressures up to 3.1 GPa have shown that T_{CDW} decreases with increasing pressure and the CDW transition is not observed at $P \geq 1.2$ GPa. T_N is approximately pressure independent.

Based on our experimental data we have assumed that in $REGe_{2.85}$ compounds (RE = Tb, Dy) T_{CDW} depends on the de Gennes factor of the rare earth element. To check this assertion we plan to synthesize new metastable compounds from the $REGe_{2.85}$ family (for example, $GdGe_{2.85}$ etc.).

TDPAC spectroscopy on *In/Cd* nuclear probes has been used to determine EFGs and magnetic hyperfine fields at probe atoms inserted in Ge lattice sites. The CDW formation in the paramagnetic phase ($T_N < T < T_{CDW}$) is accompanied by incommensurate lattice modulation, which becomes commensurate in the AFM phase ($T < T_N$). In the AFM phase Ge sites are nonequivalent, and as follows from the neutron powder diffraction, magnetic moments of Dy ions form an AFM spiral with the wave vector $\mathbf{q} = (1/2, 0, 0.164(1))$ with $\mu_{Dy} = 6.5(1)\ \mu_B$.

We assume that the CDW-PLD can lead to the distortion of the crystal structure which leads to the change of local symmetry and appearance of the antisymmetric Dzyaloshinskii-Moria exchange interaction. This interaction in turn stabilizes the spiral structure of Dy magnetic moments.

Acknowledgments

The authors are grateful to S. M. Stishov, N. G. Chechenin and V. B. Brudanin for support of this work. The work is supported by the Russian Foundation for Basic Research (Grant No. 17-02-00064) and by special program of the Department of Physical Science, Russian Academy of Sciences. The work at the Joint Institute for Nuclear Research was carried out under the auspices of a Polish representative in the JINR.

References

[1] S.S. Saxena, P. Agarwal, K. Ahilan, F.M. Grosche, R.K.W. Haselwimmer, M.J. Steiner, E. Pugh, I.R. Walker, S.R. Julian, P. Monthoux, G.G. Lonzarich, A. Huxley, I. Sheikin, D. Braithwaite, J. Flouquet Nat. 406 (2001) 587–592.
[2] A.V. Tsvyashchenko, V.A. Sidorov, A.E. Petrova, L.N. Fomicheva, I.P. Zibrov, V.E. Dmitrienko, J. Alloys Compd. 686 (2016) 431–437.
[3] J. Chang, E. Blackburn, A.T. Holmes, N.B. Christensen, J. Larsen, J. Mesot, Ruixing Liang, D.A. Bonn, W.N. Hardy, A. Watenphul, M. v. Zimmermann, E.M. Forgan, S.M. Hayden, Nature 8 (2012) 871–876.
[4] S.-W. Cheong, M. Mostovoy, Nat. Mater. 6 (2007) 13–20.
[5] C. Cao, A. Wildes, W. Schmidt, K. Schmalzl, B. Hou, L.-P. Regnault, C. Zhang, P. Meuffels, W. Loser, G. Roth, H. Li, Sci. Rep. 5 (2015) 7698.
[6] Yejun Feng, Jiyang Wang, D.M. Silevitch, B. Mihaila, J.W. Kim, J.-Q. Yan, R.K. Schulze, Nayoon Woo, A. Palmer, Y. Ren, Jasper van Wezel, P.B. Littlewood, T.F. Rosenbaum, Proc. Natl. Acad. Sci. Unit. States Am. 110 (9) (2013) 3287–3292.
[7] S. Shimomura, C. Hayashi, G. Asaka, N. Wakabayashi, M. Mizumaki, H. Onodera, Phys. Rev. Lett. 102 (2009), 076404.

[8] N. Yamamoto, R. Kondo, H. Maeda, Yoshio Nogami, J. Phys. Soc. Jpn. 82 (2013) 123701.
[9] F. Galli, R. Feyerherm, R.W.A. Hendrikx, E. Dudzik, G.J. Nieuwenhuys, S. Ramakrishnan, S.D. Brown, S. van Smaalen, J.A. Mydosh, J. Phys. Condens. Matter 14 (2002) 5067–5075.
[10] K.K. Kolincio, M. Roman, M.J. Winiarski, J. Strychalska - Nowak, T. Klimczuk, Phys. Rev. B 95 (2017), 235156.
[11] N. Hanasaki, S. Shimomura, K. Mikami, Y. Nogami, H. Nakao, H. Onodera, Phys. Rev. B 95 (2017), 085103.
[12] K.K. Kolincio, K. Gornicka, M.J. Winiarski, J. Strychalska-Nowak, T. Klimczuk, Phys. Rev. B 94 (2016), 195149.
[13] Xuetao Zhua, Yanwei Caoa, Jiandi Zhangb, E.W. Plummerb, Jiandong Guoa, Proc. Natl. Acad. Sci. Unit. States Am. 112 (2015) 2367–2371.
[14] P. Morin, M. Giraud, L.-P. Regnault, E. Roudaut, A. Czopnik, J. Magn. Magn Mater. 66 (1987) 345–350.
[15] O. Elsenhans, P. Fischer, A. Furrer, K.N. Clausen, H.G. Purwins, F. Hulliger, Z, Phys. B Condens. Matter. 82 (1991) 61–75.
[16] R.M. Galera, P. Morin, J. Magn. Magn Mater. 116 (1992) 159–168.
[17] A. Murasik, A. Czopnik, L. Keller, P. Fischer, J. Magn. Magn Mater. 213 (2000) 101.
[18] Setsuo Mitsuda, P.M. Gehring, G. Shirane, Hideki Yoshizawa, Yoshichika Onuki, J. Phys. Soc. Jpn. 61 (1992) 1469–1472.
[19] A.V. Tsvyashchenko, A.I. Velichkov, A.V. Salamatin, L.N. Fomicheva, D.A. Salamatin, G.K. Ryasny, A.V. Nikolaev, M. Budzynski, R.A. Sadykov, A.V. Spasskiy, J. Alloys Compd. 552 (2013) 190–194.
[20] A.V. Tsvyashchenko, D.A. Salamatin, V.A. Sidorov, A.E. Petrova, L.N. Fomicheva, S.E. Kichanov, A.V. Salamatin, A. Velichkov, D.R. Kozlenko, A.V. Nikolaev, G.K. Ryasny, O.L. Makarova, D. Menzel, M. Budzynski, Phys. Rev. B 92 (2015), 104426.
[21] D.A. Salamatin, V.A. Sidorov, S.E. Kichanov, D.P. Kozlenko, L.N. Fomicheva, A.V. Nikolaev, O.L. Makarova, A.V. Tsvyashchenko, Phys. Rev. B 94 (2016), 214435.
[22] A.V. Tsvyashchenko, J. Less Common. Met. 99 (L9) (1984).
[23] A.E. Petrova, V.A. Sidorov, S.M. Stishov, Phys. B 359–361 (2005) 1463–1465.
[24] V.B. Brudanin, D.V. Flossofov, O.I. Kochetov, N.A. Korolev, M. Milanov, V. Ostrovskiy, V.N. Pavlov, A.V. Salamatin, V.V. Timkin, A.I. Velichkov, L.N. Fomicheva, A.V. Tsvyashchenko, Z.Z. Akselrod, Nucl. Instrum. Meth. A 547 (2005) 389.
[25] A.V. Tsvyashchenko, D.A. Salamatin, A. Velichkov, A.V. Salamatin, L.N. Fomicheva, V.A. Sidorov, A.V. Nikolaev, A.V. Fedorov, G.K. Ryasny, V.N. Trofimov, A.V. Spasskiy, M. Budzynski, Phys. Rev. B 91 (2014), 104423.
[26] B. Lindgren, Hyperfine Interact. C1 (1996) 613.
[27] B.N. Savenko, D.P. Kozlenko, A.V. Belushkin, E.V. Lukin, S.E. Kichanov, E.S. Kuz'min, A.P. Bulkin, A.P. Sirotin, in: Proceedings of the 20th Conference on Using of Neutron Scattering in Studies of Condensed State, vol. 76, 2008.
[28] J. Rodriguez-Carvajal, Phys. B 192 (1993) 55.
[29] A. Benidris, A. Zaoui, M. Belhadj, M. Djermouni, S. Kacimi, JOSC 28 (2015) 2215–2222.